Triangular-shaped Landforms Reveal Subglacial Drainage Routes in SW Finland

Mäkinen, J.[a, *], Kajuutti, K.[a], Palmu, J.-P.[b], Ojala, A.[b] and Ahokangas, E.[a]

[a] Department of Geography and geology, University of Turku FI-20014 Turku, Finland.
[b] Geological Survey of Finland, P.O. Box 96 (Betonimiehenkuja 4) FI-02151 Espoo, Finland.
[*] corresponding author (jonmak@utu.fi).

ABSTRACT

The aim of this study is to present the first evidence of triangular-shaped till landforms and related erosional features indicative of subglacial drainage within the ice stream bed of the Scandinavian ice sheet in Finland. Previously unidentified grouped patterns of Quaternary deposits with triangular landforms can be recognized from LiDAR-based DEMs. The triangular landforms occur as segments within geomorphologically distinguishable routes that are associated with eskers. The morphological and sedimentological characteristics as well as the distribution of the triangular landforms are interpreted to involve the creep of saturated deforming till, flow and pressure fluctuations of subglacial meltwater associated with meltwater erosion. There are no existing models for the formation of this kind of large-scale drainage systems, but we claim that they represent an efficient drainage system for subglacial meltwater transfer under high pressure conditions. Our hypothesis is that the routed, large-scale subglacial drainage systems described herein form a continuum between channelized (eskers) and more widely spread small-scale distributed subglacial drainage. Moreover, the transition from the conduit dominated drainage to triangular-shaped subglacial landforms takes place about 50-60 km from the ice margin. We provide an important contribution towards a more realistic representation of ice sheet hydrological drainage systems that could be used to improve paleoglaciological models and to simulate likely responses of ice sheets to increased meltwater production.

Keywords:
Quaternary, Glaciation, Scandinavia, Geomorphology (glacial), LiDAR, Triangular-shaped landforms, Subglacial, Ice stream, Esker.

1. Introduction

The availability of high-resolution LiDAR –based DEMs (Digital Elevation Model) has enabled detailed extraction of previously unidentified glacial landforms that do not clearly adhere to current conceptions of either subglacial bedforms or glaciofluvial landforms. This paper describes a new triangular-shaped landform from southern Finland that, after studying, we argue expresses conditions of a subglacial meltwater drainage system between more widespread distributed drainage and channelized flow in conduits (eskers).

The association of distributed subglacial drainage systems (including braided canals and linked-cavity systems) with basal melting and soft, deforming bed conditions is well described in the literature (e.g. Clark and Walder, 1994; Livingstone et al., 2015). These conditions are known to dominate subglacial beds in contemporary ice streams in Antarctica (Ashmore and Bingham, 2014) and are closely linked to sedimentary rock areas within the past ice sheets (Shreve, 1985, Hooke and Fastook, 2007; Clerc et. al., 2012; Phillips and Lee, 2013; Salamon, 2015). Unfortunately, the current subglacial environments are difficult to explore and representative examples from the records of the past ice sheet beds are very sparse. As recently put by Greenwood et al. (2016a), "the apparent lack of a widespread 'distributed' system in the palaeo-record may be a product of poor preservation, or poorly developed tools and templates for identification and interpretation of non-channelized drainage". Also Livingstone et al. (2013) stated that: "Despite theoretical advances in how we understand subglacial hydrology, relatively little is known about the distribution of subglacial water and the form of the drainage system". This means that our knowledge is still largely based on theoretical glaciological reasoning and associated modeling results. Among others, distributed drainage has been modeled by Alley (1989), Humphrey (1987), Walder and Fowler (1994), Ng (2000), Flowers et al. (2003, 2004), Hewitt (2011), and Cowton et al. (2016).

The characteristics of distributed drainage system depend mainly on the ice flow rate, meltwater discharge and pressure conditions, meltwater sources (basal melt rate and water storage), as well as on the saturation and deformation of basal sediment (Beem et al., 2010). It is known that when the water pressure (Pw) increases due to the increase of discharge (Q), the drainage system is predicted to take a more distributed form and related channels to be wide and shallow (Hooke, 2005).

Importantly, the transition between a distributed drainage system and conduit system is still poorly understood and documented. The nature of the drainage system beneath the ice sheet is complex and characterized by spatial and temporal variations. The subglacial hydrology is critical when the ice stream behavior and related ice sheet dynamics as well as geomorphological records are interpreted. High subglacial water pressure and deformable beds promote low basal shear stresses that increase the flow velocities of the ice streams. However, the interactions of different sediment properties in varying subglacial environments are poorly understood. In the present paper, we simply refer to deformation till in association with the subglacial drainage in high pressure conditions (cf. Evans et al., 2006) and leave the closer analysis of the deformation processes and related water flow for future studies.

The Light Detection And Ranging (LiDAR) campaigns that produce high-resolution digital elevation models (DEM) are providing a revolutionary tool for the mapping and documentation of glacial landforms over wide areas (e.g. Johnson et al., 2015). In Finland, for example, the encompassing LiDAR data, supplemented with base maps and maps of the Quaternary deposits and bedrock, striation data, and the highest shoreline (Ojala et al., 2013) provide an excellent opportunity to explore the ice stream bed features and related dynamics of the past Scandinavian ice sheet with resolution that has not been possible with earlier research data and methods.

The aim of this study is to present the first evidence of triangular till landforms and related geomorphic features indicative of subglacial drainage routes within the ice stream bed of the Scandinavian ice sheet in Finland. We discuss geomorphological characteristics of the drainage systems and their sedimentology, providing examples from the Baltic Sea ice lobe area in SW Finland. Importantly, we endeavor to provide a link between distributed drainage and conduit systems (eskers) with wider implications for the ice stream hydrology as well as for the deglacial ice stream dynamics.

2. Study area

The study area is located in southwestern Finland, between the Salpausselkä III (Ss III) ice-marginal zone and about 45 km long stretch of the Bothnian Sea coast north of the city of Pori (Fig. 1). Major interlobate eskers of Somero-Pori and Pälkäne-Tampere delimit the study area in southwest and northeast, respectively. Towards the northwest the Pälkäne-Tampere interlobate esker is replaced by the western arc of the Central Finland Ice-Marginal Formation (CFIMF, Fig. 1). The bedrock of the area consists mostly of Precambrian crystalline rocks with Paleoproterozoic intermediate volcanic rocks in the east, and Paleoproterozoic migmatites, gabbros, paragneisses and granitoids in the central area and in the north. Mesoproterozoic sandstones appear in the western sector of the study area (Lehtinen et al., 2005) (Fig. 1).

The area has been repeatedly glaciated during the late Quaternary by the Scandinavian Ice Sheet (SIS) as reviewed by Lunkka et al. (2004), Saarnisto and Lunkka (2004) and Svendsen et al. (2004), among others. As a consequence, glacial and glaciofluvial superficial deposits are typical features of the landscape. These deposits reflect several types of glacial deposition environments that are spatially well defined around the study area. The northern part has a more distinct terrain relief, bedrock outcrops are frequent and superficial deposits are thin (Fig. 2). Towards the west the bedrock-dominated relief changes to more till-dominated terrain that is characterized by low-relief hummocks and ribbed moraines known as Satakunta hummocky moraine terrain (HMT) (Fig. 1). In the Pori area, Mesoproterozoic sandstones are covered by anomalously thick beds of Quaternary sediments. In the central part (to the SE of the Satakunta HMT), NW to SE oriented esker systems (Fig. 1) and elongated streamlined ridges, drumlins and moraine complexes are common.

The Ss III ice-marginal zone in the SE sector consists of discontinuous marginal till ridges as well as several prominent marginal deltas, and feeding esker systems. Thicker superficial deposits, covered by the post-glacial fine-grained sediments (silt and clay) are filling the rolling relief in the southern part of the study area.

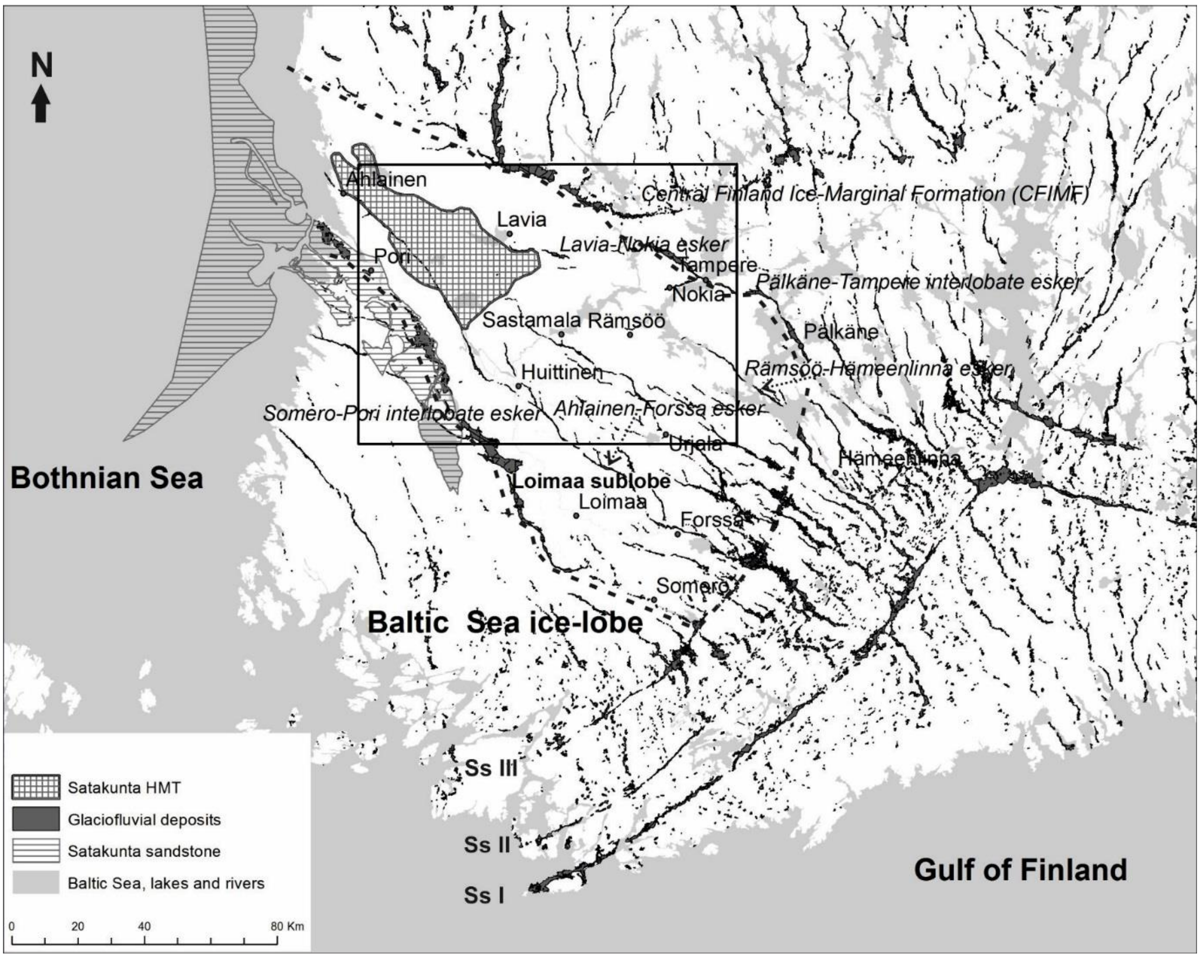

Fig. 1. Location of the study area. The study area (Loimaa sublobe) is delineated with dashed line including the Satakunta hummocky moraine terrain (HMT) as indicated in the map of Quaternary deposits 1:1 000 000 (Geological Survey of Finland, 2016). The study area is bordered by the Salpausselkä III ice-marginal complex, the Somero-Pori and Pälkäne-Tampere interlobate eskers as well as the western part of the Central Finland Ice-marginal Formation. The area in Fig. 2 is indicated by a box. The Loimaa sublobe represents the eastern margin of the Baltic Sea ice lobe that became separated from the main lobe during the deglaciation. Ss I-III refer to Salpausselkä Younger-Dryas ice-marginal complexes. Basemap © National Land Survey of Finland. (2 column image)

The Weichselian deglaciation from the last glacial maximum (LGM) started soon after 20 ka ago, and by the colder period known as the Younger Dryas (YD, 12.9-11.7 ka ago), the ice margin had already retreated to the Salpausselkä region in southern and eastern Finland. The deglaciation of the present study area took place during the early Holocene between ca. 11.5 and 11.0 ka ago (Svendsen et al., 2004; Hughes et al., 2016; Stroeven et al., 2016).

Large ice-marginal complexes, esker systems and interlobate formations indicate that the SIS was divided into several ice lobes during the deglaciation (Boulton et al., 2001; 2009). The present study area covers the eastern part of the Baltic Sea ice lobe that was characterized by perennial streaming activity through the Bothnian Sea and terminated at the arcs of Salpausselkä (Ss) ice-marginal complexes (Fig. 1). The dominant SE-NW fan-shaped flow direction (270-340°) of the Baltic Sea ice lobe in Finland is rather well known based on the evidence from lineation and striations, directions of eskers and De Geer moraines as well as glacial transport of surface boulders (Kujansuu and Niemelä, 1984; Salonen, 1986; Ojala, 2016).

During the rapid deglaciation after the formation of the Ss III, the eastern margin of the Baltic Sea ice lobe formed the minor Loimaa sublobe that was bordered in the west by the Somero – Pori interlobate esker (Mäkinen, 2003a) (Fig. 1). The deglaciation was fast with the ice-marginal retreat rate of about 300-400 m/yr. (cf. Sauramo, 1923) and with only minor ice-marginal deposits to the NW of the Ss III. It is noteworthy that we have recently suggested the existence of the Urjala-Akaa subglacial lake (ca. 100 km^2) about 50 km from the Ss III ice-marginal complex (Kajuutti et al., 2016) (Fig. 1). This lake seems to be associated with the southernmost triangular landforms described in this paper (Fig. 2).

The final stages of the Loimaa sublobe were related to the complex landform patterns of the Satakunta hummocky moraine terrain that is characterized by the absence of eskers. The Ahlainen - Forssa esker follows the western side of the hummocky moraine terrain (Fig. 1). The deglaciation in the study area occurred mostly in a subaquatic environment with the proglacial water depths of 10 – 50 m in the east and up to 200 m in the west, except for minor supra-aquatic areas around the Ss III (Ojala et al., 2013).

3. Materials and methods

The study was mainly based on analysis of LiDAR-derived airborne DEMs, topographic maps, aerial photographs, and geological and aerogeophysical mapping dataset available at Maankamara map service (http://gtkdata.gtk.fi/maankamara/) of the Geological Survey of Finland (GTK). The LiDAR-based point cloud data (0.5 points per square meter) was processed at GTK in order to create a 2-meter grid DEM. Mainly two types of DEM visualizations were used: (i) MDOW, which incorporate a multidirectional, oblique-weighted hill shade (Jenness, 2013) and (ii) a slope theme that was accessed dynamically from the DEM data. For the MDOW, we used a primary illumination direction of 315° and a vertical exaggeration factor of four. The MDOW and slope data layers were typically incorporated with transparency settings of 50 % for both themes. Data processing and visualization were done with the ArcGIS (©ESRI) software.

Most sites with interesting morainic landforms were visited during the field work in autumn 2016. The field reconnaissance included visual examination, photographing and description of till deposits, but the sites were not extensively excavated during the present study. However, where available, the GTK database of their test pits was accessed to examine the internal stratigraphy in a number of key locations. In addition, one roadside pit (Harjakangas S) was logged for sedimentology and a few fresh road excavations were examined for sediment characteristics.

4. Results

4.1. Triangular-shaped landforms and related features

Previously unidentified grouped patterns of Quaternary deposits forming triangular-shaped landforms can be easily recognized from LiDAR-based DEMs (Figs 3-5). The triangular landforms consist of till and are variously associated with the more complex patterns of fan-shaped hollows and diagonal or slightly curved low escarpments, small longitudinal or winding till ridges, irregular hummocks and channel-like passages.

The triangular landforms are poorly detectable from map contour-lines, other remote sensing images and even in the field within forest covered areas. For the present study area 23 sites with distinct areas of triangular landforms were recorded (Tables 1 and 2; Fig. 2).

Table 1
Sites with triangular landforms (see Fig. 2). Coordinates (X, Y) are according to ETRS-TM35FIN system. Route = the site belongs to a geomorphologically distinguishable route, Esker = the site joins an esker, the site with x without parentheses is closest to a start of an esker, Valley = the site is associated with a bedrock fracture valley, HM = the site is located within a previously mapped hummocky moraine area, the site with x without parentheses indicates that triangular landforms have been previously classified as hummocky moraine. No x means that the triangular landforms have been marked as ground moraine.

Site	**Site name**	**X**	**Y**	**Route**	**Esker**	**Valley**	**HM**
1	Poosjoki	225984	6846624	x	(x)		(x)
2	Harjakangas N	234352	6837332	x	(x)		x
3	Harjakangas S	236288	6834256	x	(x)		x
4	Puhju	233608	6829700				x
5	Joutsijärvi	242968	6827108	x	(x)		(x)
6	Sääksjärvi W	247280	6819916	x	(x)		(x)
7	Sääksjärvi N	254864	6822056	x	(x)		(x)
8	Sääksjärvi E	260712	6819324	x	x		x
9	Lievijärvi	261792	6812534		x		x
10	Ylistenjärvi W	278012	6797334	x	(x)		
11	Ylistenjärvi S	281184	6794710	x	x		
12	Kynäsjärvi W	245620	6851874	x	(x)		(x)
13	Kynäsjärvi E	251240	6848498	x	(x)		(x)
14	Lehmijoenkylä	253816	6846318	x	(x)		(x)
15	Jokihaara	259984	6841594	x	x	x	(x)
16	Murtoo	300688	6810197		x	x	
17	Joenpohja	307520	6807014		x	x	
18	Saastojärvi	304352	6799418			x	x
19	Enonkulma	296984	6797758				
20	Kyrkönmaa	299160	6793806				(x)
21	Ameenjärvi	306544	6792854		x		
22	Kikuri	308604	6788806				
23	Hopeavuori	337860	6779434		x		

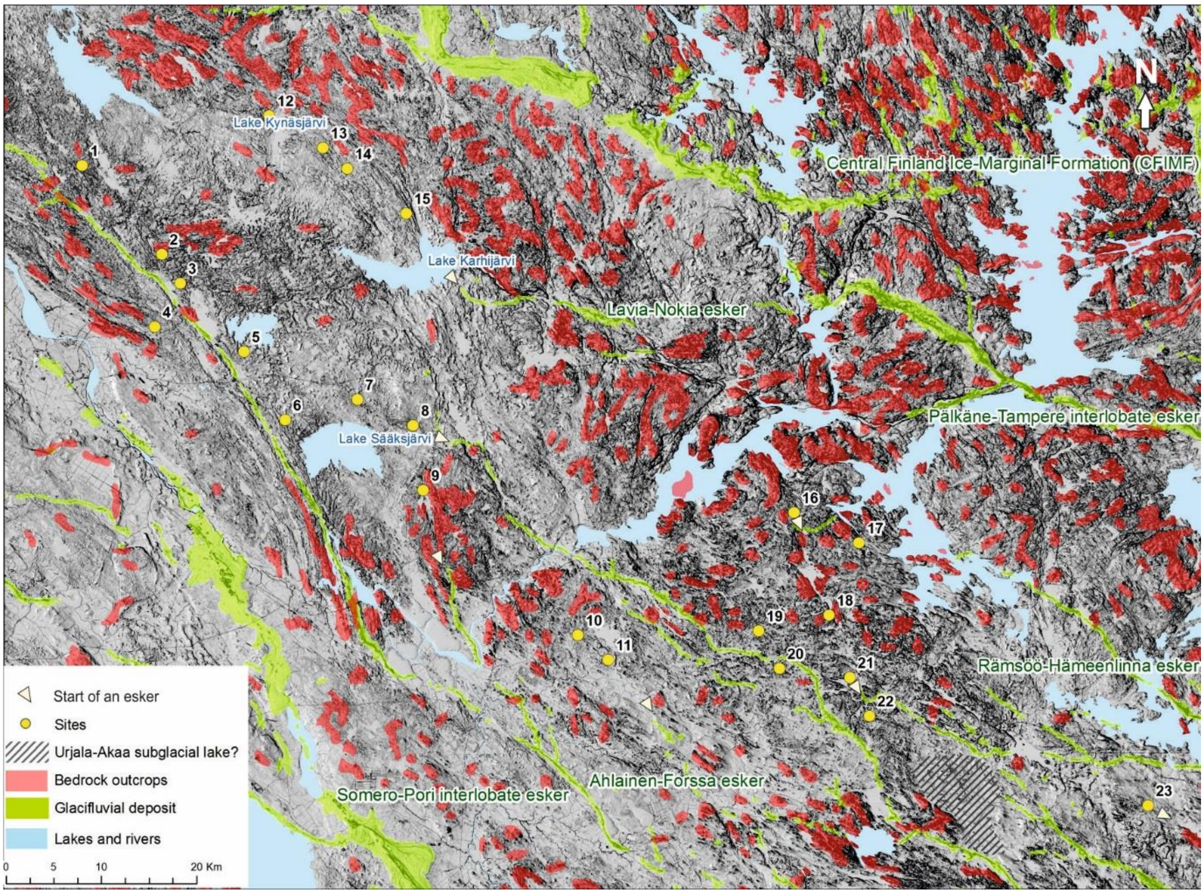

Fig. 2. Location of triangular landforms within the study area (see Fig. 1). The study area in the image is delineated by the Somero-Pori and Pälkäne-Tampere interlobate eskers as well as the western part of the Central Finland Ice-marginal Formation. Sites refer to places selected on the basis of occurrence of grouped triangular landforms (see Table 1 for sites). The sites constitute the following routes associated with a start of an esker: Poosjoki-Sääksjärvi (sites 1-3, 5-6, 9), Kynäsjärvi-Jokihaara (sites 12-15), Sääksjärvi (sites 7-8) and Ylistenjärvi (sites 10-11). Basemap and LiDAR © National Land Survey of Finland. LiDAR processing © Geologian tutkimuskeskus. (2 column color image)

Topographically, the triangular landforms occur in the areas with overall minor relative height differences. Furthermore, they are located either on the upstream (ice flow) side of the bedrock fracture valleys or in the down-hill areas of the low-relief bedrock highs. On the maps of Quaternary deposits these landforms have been earlier mapped as moraine ridges and hummocky moraines or ground moraine (Kujansuu and Niemelä, 1984).

Importantly, the triangular landforms occur as segments within geomorphologically distinguishable routes (Figs. 3 and 4) that have down-ice association with eskers (Fig. 2). We therefore refer to distributed drainage routes. The two longest routes are the Poosjoki-Sääksjärvi (sites 1-3 and 5-6, length 40 km) and the Kynäsjärvi-Jokihaara route (sites 12-15, length 25 km), and they form the margins of the Satakunta hummocky moraine terrain. Near the lake of Sääksjärvi (formed by a meteorite) the Poosjoki-Sääksjärvi route becomes divided forming the shorter Sääksjärvi route (sites 7-8, length 15 km). The Poosjoki-Sääksjärvi route likely continues about 15 km through the crater lake until site 9 (Fig. 2). The Kynäsjärvi system (Figs. 3A and 5) represents the most characteristic site of the triangular-shaped landforms in the present study area. In general, the orientation of the triangular features matches with the latest ice flow direction, pointing towards east/south-east.

Table 2
Appearance of the triangular landforms in the study sites (see Table 1 and Fig. 2).

Site	Description
1	sparse triangular forms, complex forms, large marginal (SW) fan-shaped hollows.
2	large fan-shaped hollows and triangular forms, spreading of the route towards E.
3	triangular and complex forms, fan-shaped hollows, spreading of the route towards E.
4	few weakly developed and elongated triangular forms, fan-shaped hollows, within basement rock shear zone, 4-5 km from the esker.
5	small till ridges and channel like passages with transition to small triangular forms, complex forms, spreading of the route towards SE in association with large hummocky moraine/lunate hummocks.
6	well-developed triangular forms, two branches, large fan-shaped hollows and triangular landforms, eastern branch with complex forms.
7	well-developed triangular forms with change in sharpness of slopes across the route, partly complex forms, fan-shaped hollows, weak connection to site 5.
8	mainly complex forms with few triangular forms, associated with site 7 and an esker.
9	triangular forms with hummocky appearance, fan-shaped hollows, between site 6 (separated by a meteorite crater lake) and an esker.
10	mainly small triangular forms associated with small till ridges, fan-shaped hollows.
11	small triangular forms with small till ridges, fan-shaped hollows.
12	well-defined triangular forms with change in sharpness of slopes across the route, fan-shaped hollows.
13	mostly weakly developed and elongated triangular landforms, fan-shaped hollows, low escarpments complex forms, widening route towards SE.
14	few triangular forms, fan-shaped hollows, complex forms, low escarpments.
15	few triangular forms, transition to till ridges and low escarpments.
16	few triangular landforms, transition to low escarpments (terraces).
17	few triangular landforms, fan-shaped hollows, transition to low escarpments /winding till ridges (terraces).
18	few triangular landforms, transition to low escarpments (terraces).
19	few weakly developed triangular landforms, fan-shaped hollows, complex forms.
20	few weakly developed triangular landforms and fan-shaped hollows, within bedrock knob lee sides.
21	few triangular landforms, downstream transition from bedrock channel to fan-shaped hollows and triangular landforms and finally to an esker
22	scattered few triangular landforms between two eskers, upstream from the suggested Urjala-Akaa subglacial lake
23	few triangular landforms and fan-shaped hollows, complex forms, between large hummocky/ribbed moraines and an esker, downstream from the suggested Urjala-Akaa subglacial lake.

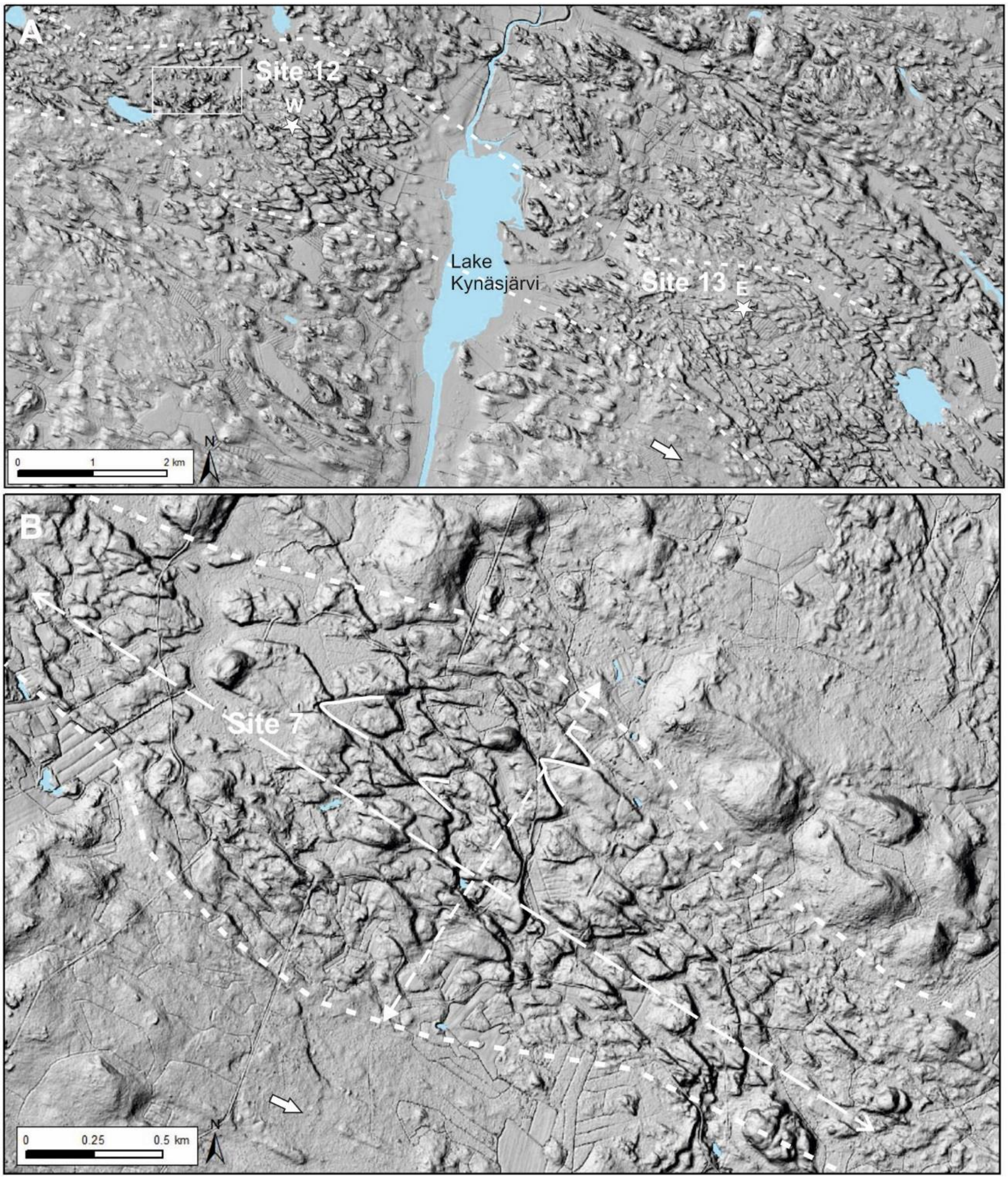

Fig. 3. The geomorphologically distinguishable routes with triangular landforms. (A) the Kynäsjärvi sites (12-13). The stars (W and E) refer to the test pit sites by the Geological Survey of Finland (see Fig. 12). After the Kynäsjärvi E site, the route becomes more spread and less well defined towards SE. The area shown with a rectangle has several bedrock outcrops along the route just before the characteristic triangular till geomorphology of the Kynäsjärvi W site. A white arrow indicates the ice flow direction. (B) The Sääksjärvi N site (7) characterized by the triangular landforms and fan-shaped hollows (some of them indicated by curved lines). Note the similarities with the Kynäsjärvi W site including the transverse change of erosional slopes across the route with most incised pattern in the middle (dashed arrow, see Figs 5A and 7). The profiles perpendicular and parallel to the route (dashed arrow) are shown in Fig. 7. A white arrow indicates the ice flow direction. Basemap and LiDAR © National Land Survey of Finland. LiDAR processing © Geologian tutkimuskeskus. (2 column image)

Some triangular landforms exist along minor and less continuous routes like the Ylistenjärvi route (sites 10-11, length 10 km) to the SE of the Satakunta HMT (Figs 2 and 4). In addition, they also exist in relation to the major bedrock fracture valleys associated with eskers (sites 16-18, Fig. 2). The southernmost triangular landforms (sites 19-23, Fig. 2) occur at the eastern margin of the central esker network and close to the proposed Urjala-Akaa subglacial lake about 50 km from the Ss III ice-marginal complex (cf. Kajuutti et al., 2016). Furthermore, there exist some scattered triangular-like features with poorly defined patterns that have not been marked into figure 2, which indicates that there is a continuum from poorly to well-developed triangular landform assemblages.

Additionally, between sites 2-5 and 13-15 there occurs spreading of the distributed drainage routes with triangular landforms (Table 2). The spreading at sites 2, 3 and 5 seems to be associated with ribbed moraines, whereas sites 13-15 show down-ice transition to longitudinal or slightly curved till ridges mapped earlier as hummocky moraines. In these cases, however, the definition of the route boundaries is somewhat difficult.

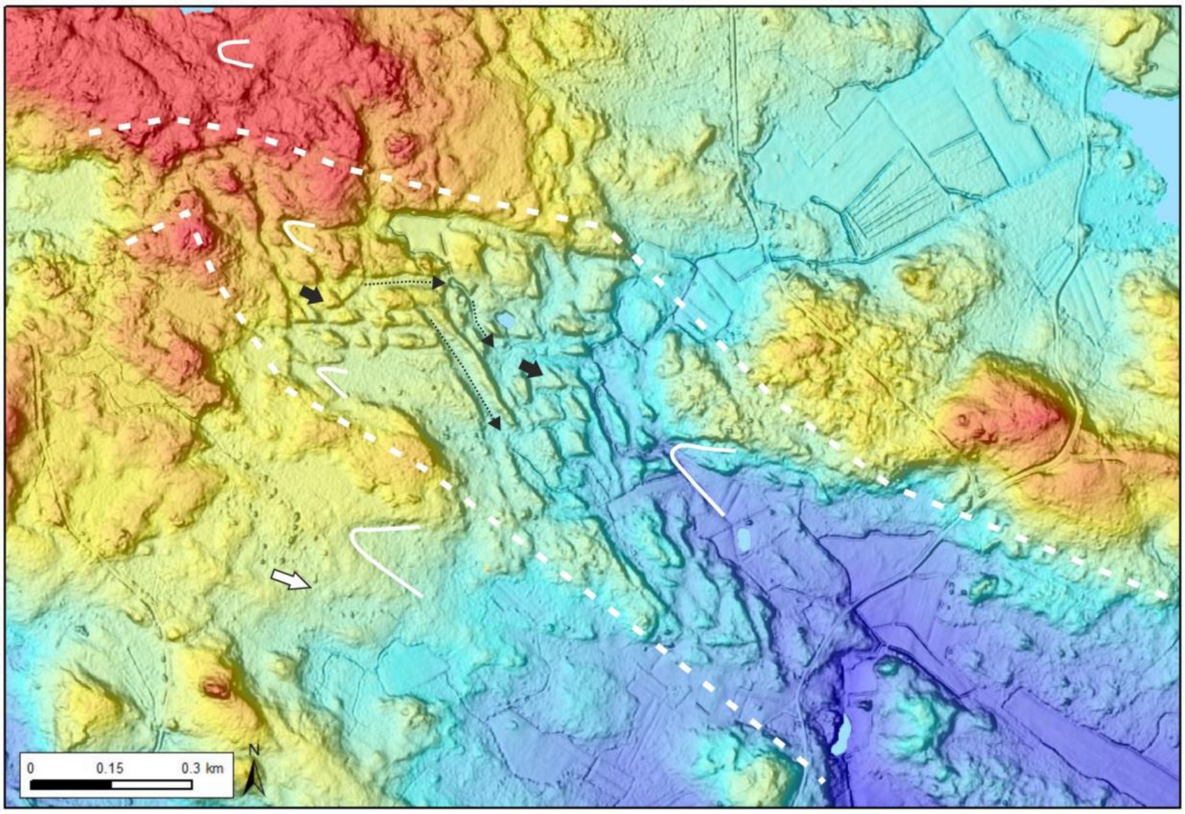

Fig. 4. The short Ylistenjärvi route (Fig 2, site 10). The route shows mainly small triangular forms (short arrows) associated with small till ridges separated by channel-like passages (pointed arrows). The route goes across a bedrock high (in NW). Note the different fan-shaped hollows (solid curves); the ones outside the route with less erosional sides, whereas those within the route reveal sharper erosion. Colors indicate decreasing

altitude from red (> 100 m asl) to blue (< 90 m asl). A white arrow shows the ice flow direction. Basemap and LiDAR © National Land Survey of Finland. LiDAR processing © Geologian tutkimuskeskus. (2 column color image)

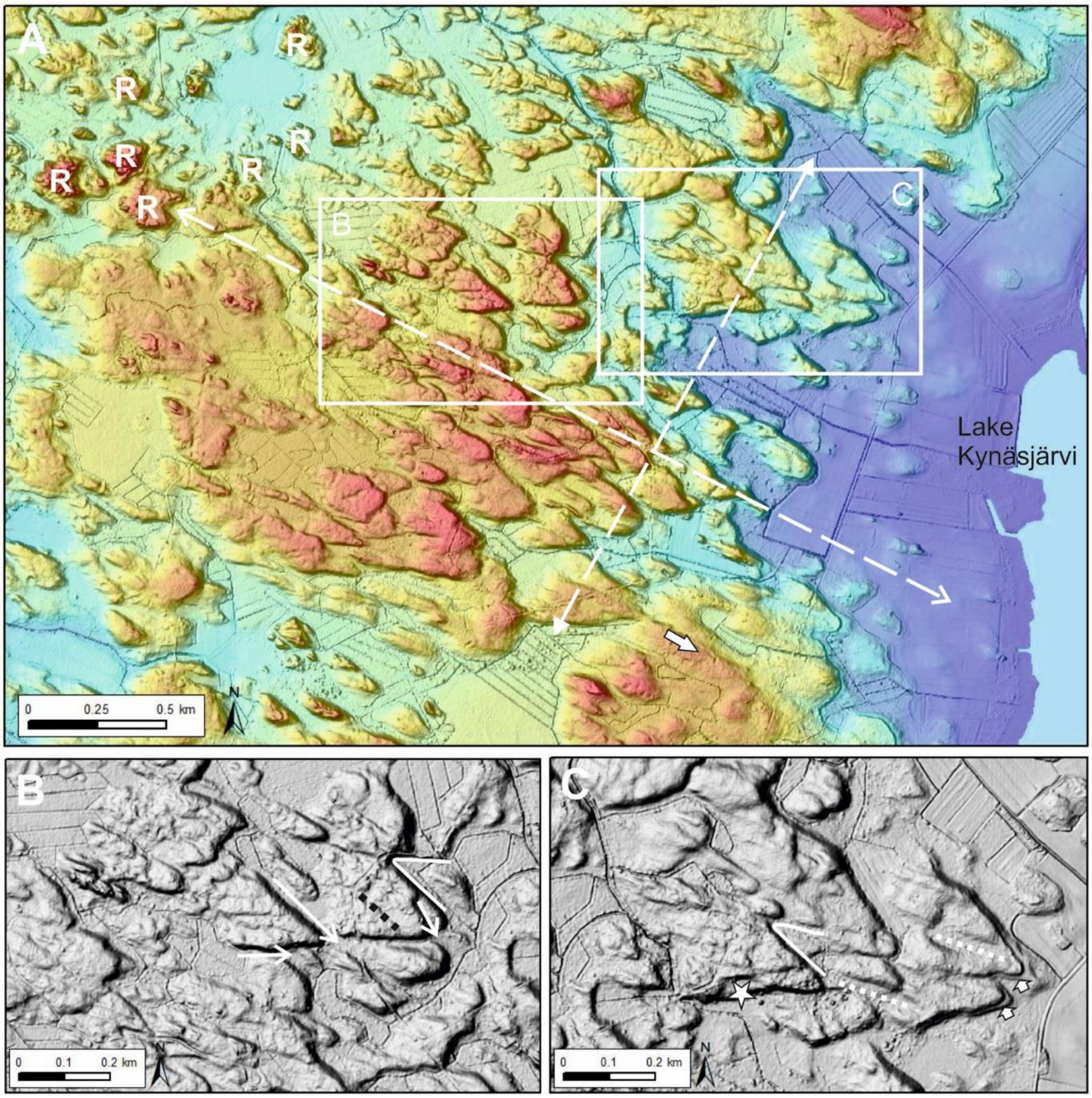

Fig. 5. The Kynäsjärvi W site (12). (A) The site is composed of several triangular-shaped till deposits. Note the morphological change of the triangular landforms across the field (dashed SW-NE arrow, cf. Fig. 7) and the more complex pattern in the middle. The triangular landforms are more sharply incised towards NE. Letters R indicate bedrock outcrops upstream of the triangular landforms. A dashed NW-SE arrow refers to the longitudinal profile in Fig. 7. A white arrow indicates the ice flow direction. Colors indicate decreasing altitude from red (> 70 m asl) to blue (< 60 m asl). (B) Arrows indicate diagonal and erosional slopes across the triangular forms, and a dashed black line is drawn along a boulder ridge. A solid curve refers to a fan-shaped hollow (C) White dashed lines point to elongated erosional surfaces and short arrows indicate the terraced ancient shoreline of the lake Kynäsjärvi. The star refers to Fig. 6A. Basemap and LiDAR © National Land Survey of Finland. LiDAR processing © Geologian tutkimuskeskus. (2 column color image)

4.2. Morphology of the triangular landforms and related features

The triangular landforms are typically 100-200 m long and their shallow proximal part is usually as wide as the landform is long. However, in some cases they are more elongated with length:width ratio reaching to 2:1. The smallest triangular features are about 40 m in size, while the largest ones can reach 300-400 m. The down-ice margins of triangular landforms show steep slopes varying between 20-30 degrees (Fig 6A-D) and are commonly boulder-rich with occasional larger erratics. Generally, the height of the slopes in distal part reaches 2-5 m, but can be up to 10 m in some cases.

The triangular landforms can side-lap each other forming interlocking features (Fig. 5). Larger features are often superimposed by smaller ones or diagonal terraces (cut-offs) representing a secondary triangular head. The surfaces are frequently boulder-rich and characterized by small and short boulder ridges on top of the landforms (Fig. 6 E-F), as well as low channels or hollows, and occasionally more complex and irregular patterns. These boulder ridges are not seen in the LiDAR DEMs, but they were distinctly distinguished during the field work. The bottom of the down-ice slopes often reveals boulder surfaces and cavities around large boulders.

The most distinct areas with triangular landforms within the Baltic Sea ice lobe are typically 1.0-2.5 km wide and continue 1.0-4.0 km in length. A change in the triangular landform morphology across the route at the Kynäsjärvi W site (Fig. 5A) depicts the particular and typical fingerprint these systems often have. The central part of these systems shows the sharpest and steepest down-ice margins associated with denser pattern of channel like passages, whereas the marginal landforms have more rounded down-ice margins and more gentle surface morphology (Figs 4 and 5A). Bedrock exposures were not encountered within the triangular landforms during the field control although bedrock outcrops are common along the routes.

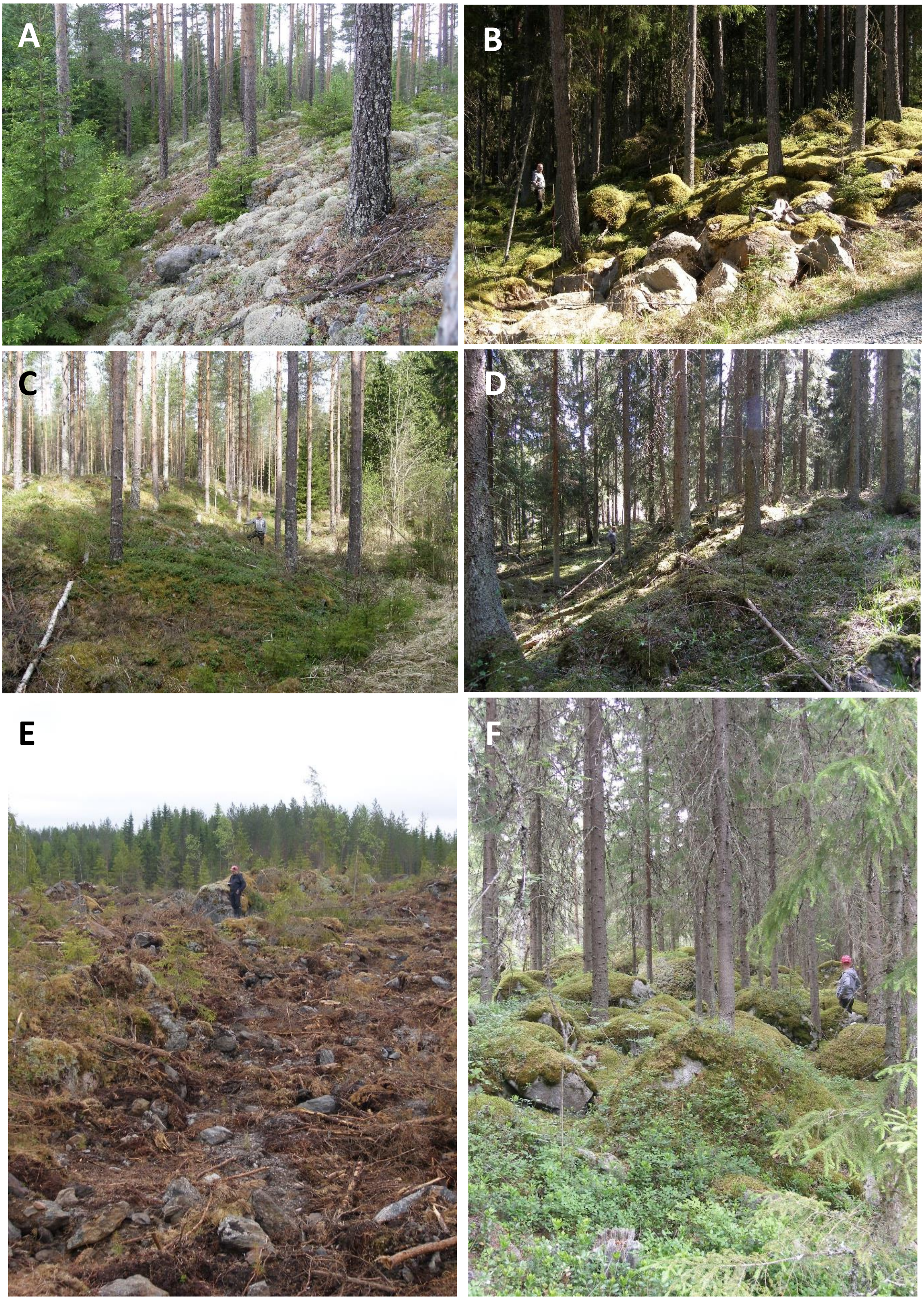

Fig. 6. Marginal down-ice slopes and small boulder ridges of the triangular landforms (A) The slope of a triangular landform in the Kynäsjärvi W site (12, see Fig. 5C) (B) The boulder-rich low escarpment within the Murtoo system (C) The slope of a triangular landform in Sääksjärvi N site (7). Note the person for scale (D) The low escarpment within the Murtoo system (site 16) facing towards a bedrock fracture valley (E) The bouldery surface of a triangular landform in Fig 5B with a boulder ridge behind a person in the Kynäsjärvi W site (12) (F)

A boulder ridge alongside of a triangular landform within the Murtoo system (site 16, cf. Fig. 11). © Photographs by Kari Kajuutti. (2 column color image)

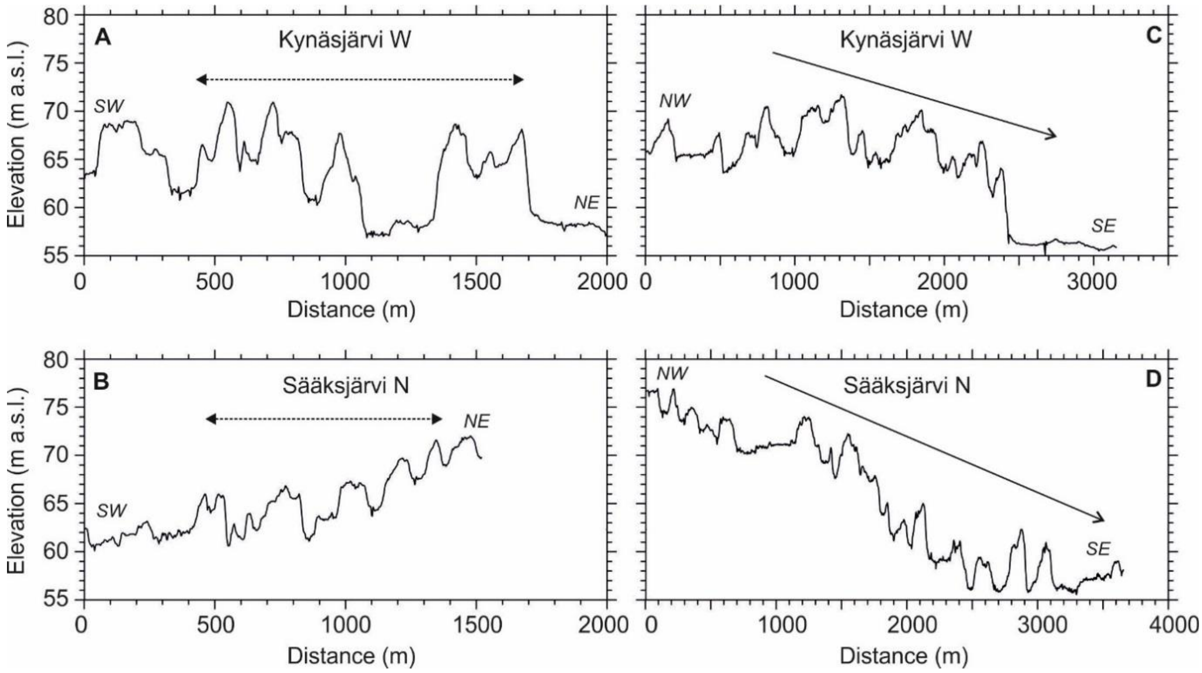

Fig. 7. Profiles of the triangular landform areas from the Kynäsjärvi W (site 12) and the Sääksjärvi N (site 7) . Cross sections (A and B) with an arrow indicating the area of the triangular landforms, and longitudinal sections (C and D) with an arrow indicating the downhill decrease in the altitude of the triangular landforms. (2 column image)

The triangular landforms are frequently associated with fan-shaped hollows and in few places with small till ridges and channel-like passages (Figs 3B, 4, 8 and 9). The fan-shaped hollows are opening down-ice and often show prolonged low escarpments, and form complex patterns indicating partial preservation. They are also associated with pull-apart till blocks of varying morphology, and their proximal head is often joined by a channel (Fig. 8). These hollows vary in size and are at their largest and most pronounced in the Sääksjärvi W site (6) (Fig. 8).

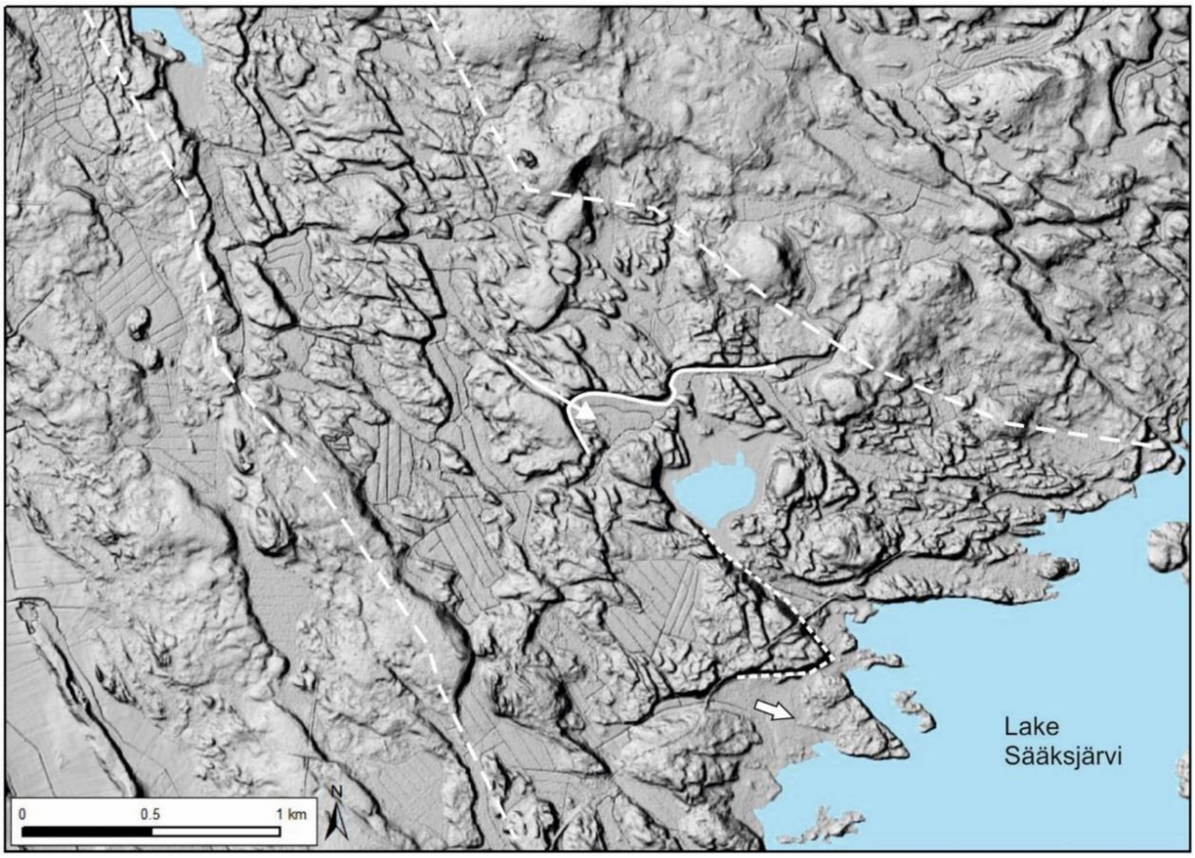

Fig. 8. The well-developed triangular landforms in the Sääksjärvi W site (6). The largest triangular landform observed (slope height about 10 m, short dashed line) and large fan-shaped hollows (solid curves) within the route (delineated by dashed lines). Note a shallow channel joining the upstream head of a fan-shaped hollow. A white short arrow indicates the ice flow direction. Basemap and LiDAR © National Land Survey of Finland. LiDAR processing © Geologian tutkimuskeskus. (2 column image)

The special feature on the eastern side of the Kynäsjärvi W site (12) is the terraced down-ice margins of the side-lapping triangular landforms (Fig. 5C). The terrace slopes are boulder-rich with slope angles between 10-20 degrees. The size of the terraces is about 3-5 m in width and 1-2 m in height. These terraces represent the old shoreline of the Kynäsjärvi Lake before the 3.9 m artificial lowering of the lake level at the end of 19th century (cf. Kangas, 2003).

In the Ameenjärvi site (21), the triangular landforms and fan-shaped hollows are part of the landform change from subglacial erosional channels to an esker (Fig. 9). This site provides a good example of how the triangular landforms are related to the subglacial meltwater flow.

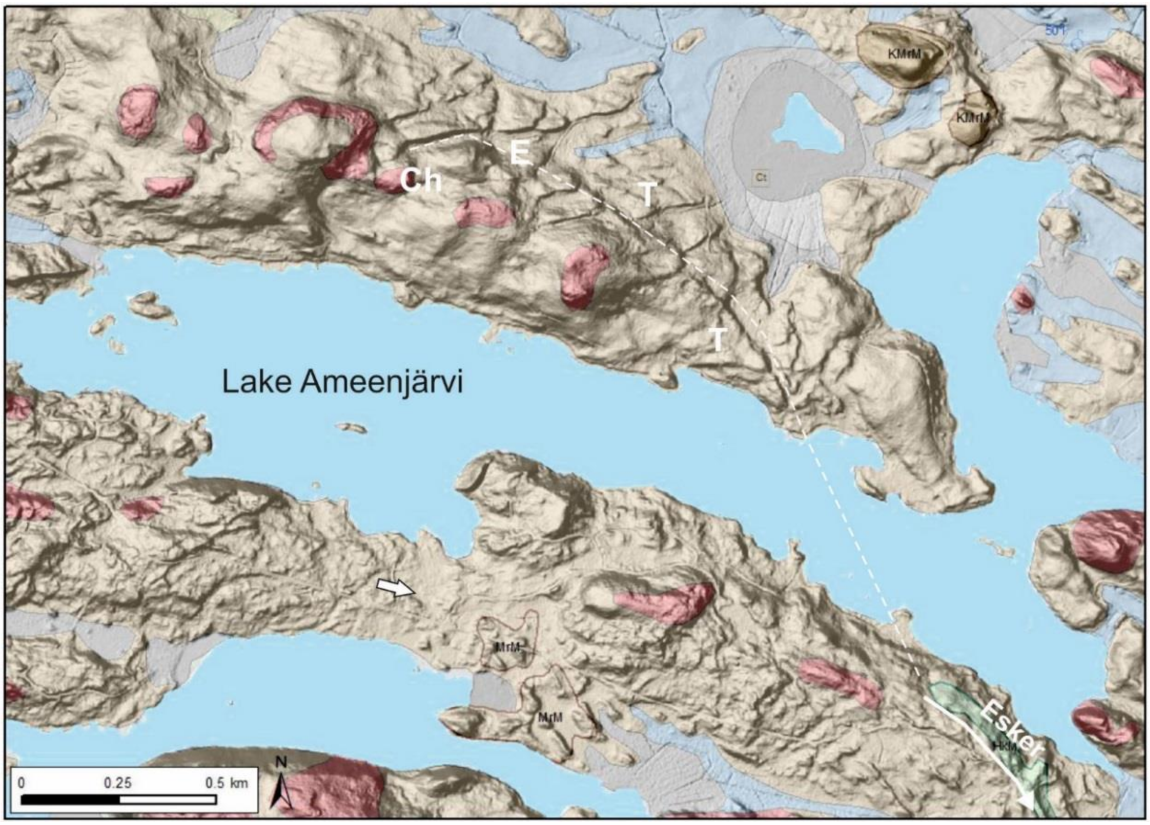

Fig. 9. The Ameenjärvi site (21) on a map of Quaternary deposits. The site reveals a landform change (dashed line) from an erosional channel (Ch), to triangular landforms (T) and fan-shaped hollows (E) and finally to the start of an esker. Exposed bedrock is shown with red, hummocky moraines with dark brown, ground moraine with brown and an esker with green color. A white short arrow indicates the ice flow direction. Basemap and LiDAR © National Land Survey of Finland. LiDAR processing © Geologian tutkimuskeskus. (2 column color image)

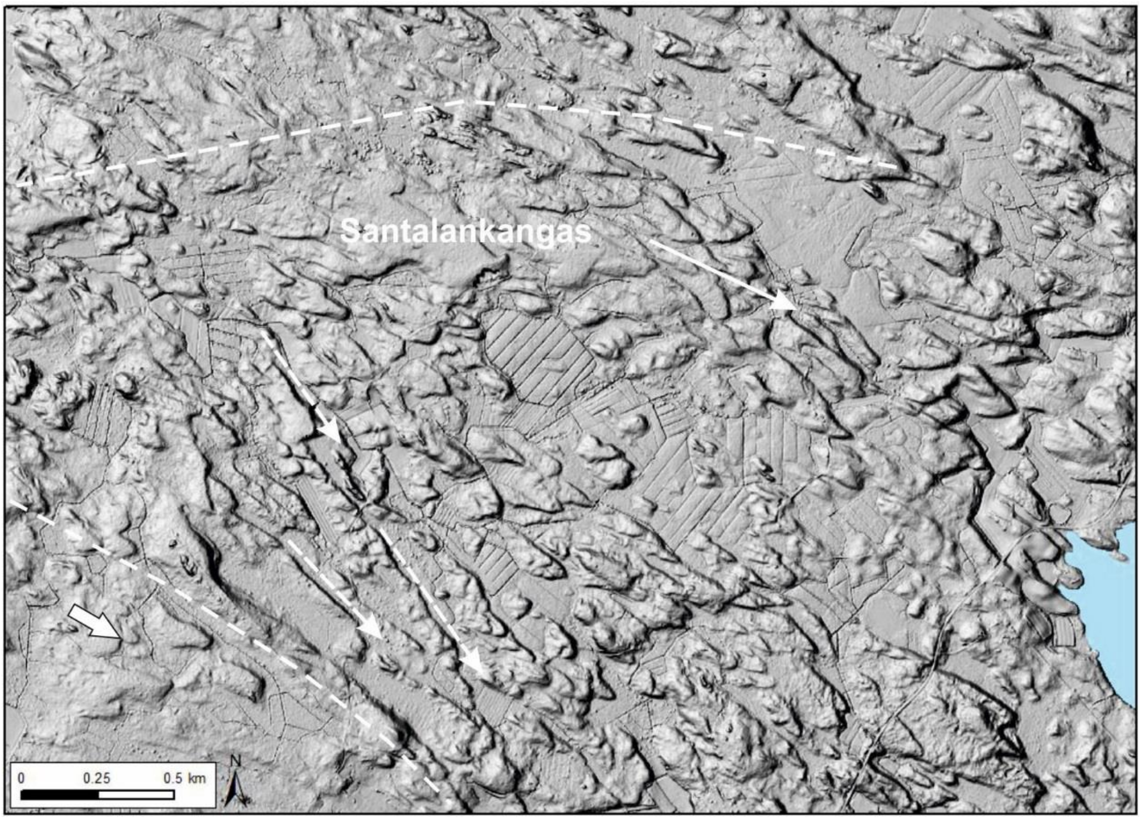

Fig. 10. The Kynäsjärvi E site (13, Santalankangas). The area shows the complex pattern of narrow and more elongated triangular features (solid arrow), low escarpments and channel-like passages (dashed arrows). The SW margin of the route (delineated by dashed lines) is better defined than the NE side. A white arrow indicates the ice flow direction. Basemap and LiDAR © National Land Survey of Finland. LiDAR processing © Geologian tutkimuskeskus. (2 column image)

The triangular landforms are sometimes associated with diagonal or slightly curved low escarpments (Figs 10 and 11). These are either low ridges with an erosional slope on the other side or terraces that can be from few hundreds of meters up to few kilometers long. Similar to triangular landform slopes, they show 2.5-5 m high steep slope with angles ranging between 20-30 degrees, and are also associated with boulder belts. The low escarpments with often terraced morphology typically occur along the margins of bedrock fracture valleys sheltered from the ice flow. Moreover, to the upstream a change to triangular features can be found as exemplified by the Murtoo system (site 16, Fig. 11).

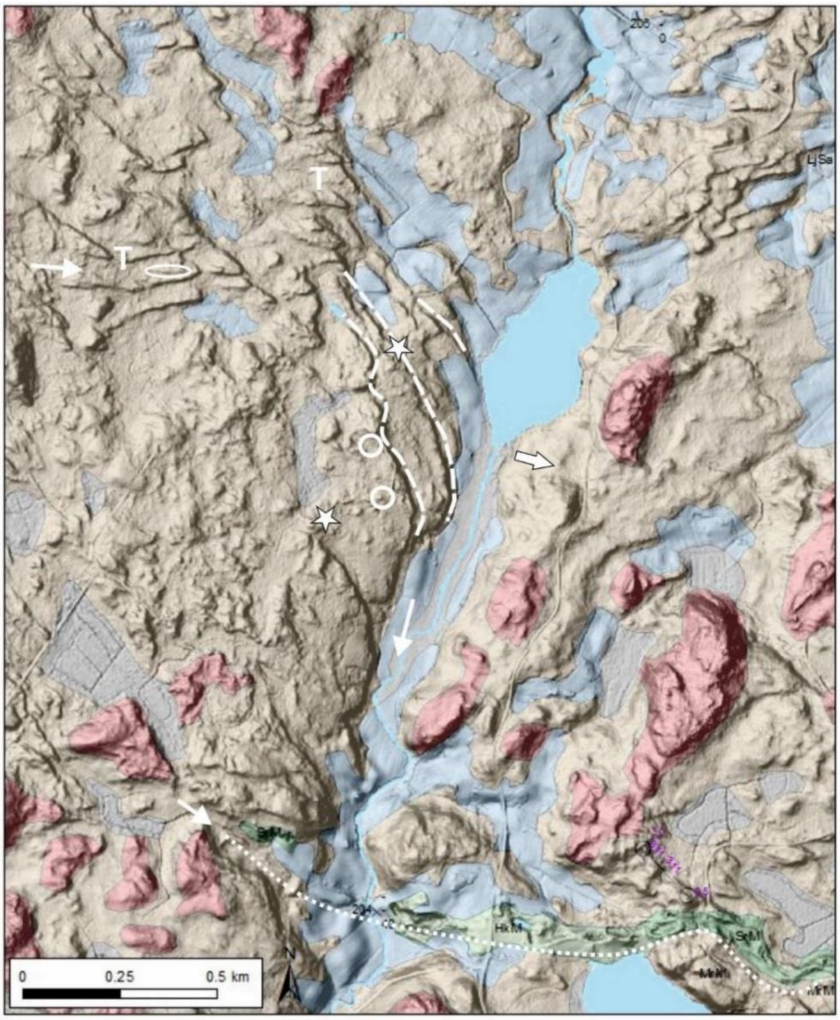

Fig. 11. The Murtoo system (site 16) on a map of Quaternary deposits. Red colour is for bedrock, brown for till (till), green for sand/gravel (esker), and blue for clays. Note the transition from triangular landforms (T) to low escarpments (dashed lines) along the side of a bedrock fracture valley towards the start of the Ramsöö – Hämeenlinna esker (pointed line). Stars refer to roadside cuts with clayey till, whereas circles show cuts with sandy tills. A boulder rich small ridge on a triangular landform is shown with solid oval-shaped line (Fig. 6F). White arrows indicate meltwater flow, whereas a thicker arrow indicates the ice flow direction. Basemap and LiDAR © National Land Survey of Finland. LiDAR processing © Geologian tutkimuskeskus. (1,5 column color image)

4.3. Sedimentology of the areas with triangular landforms

The sedimentology of the triangular landforms is based on several test pits, sediment logs, and grain-size analysis made by GTK within the Satakunta hummocky moraine terrain in 1986 (Fig. 12). Based on these, the tills of the triangular landforms are mainly composed of structureless (sometimes associated with sand or gravel patches) or slightly deformed (gneissic structure), sandy and gravelly tills with low mud content.

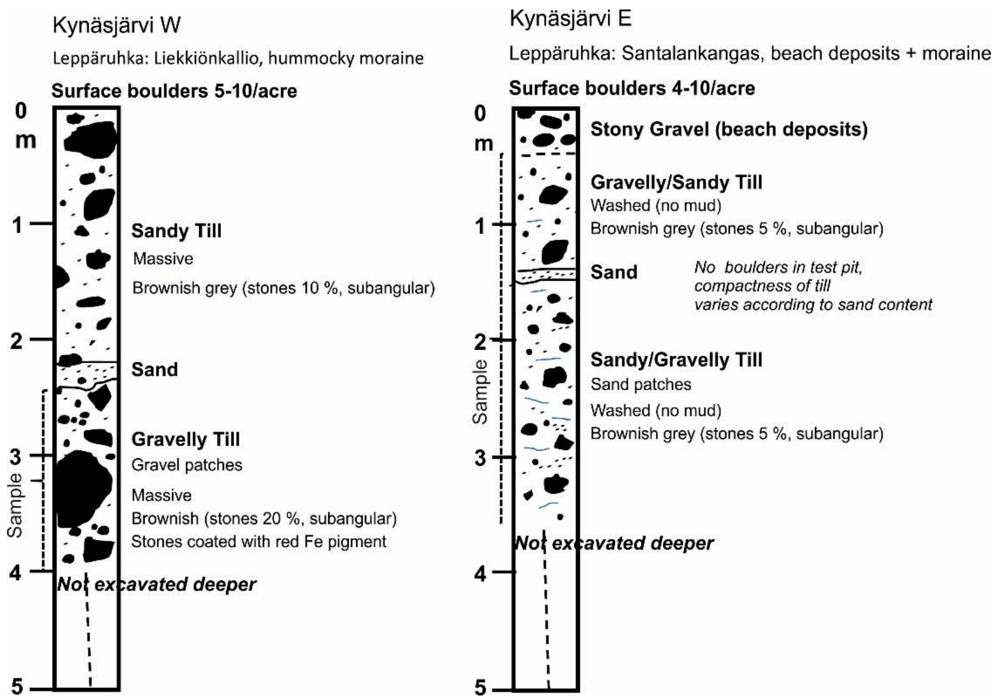

Fig. 12. Sedimentological logs from the Kynäsjärvi W and E sites (12 and 13, Fig. 2). The logs are based on the test pit drawings/descriptions by the Geological Survey of Finland in 1986. Note the intervening sand layers between different till beds. (1,5 column image)

The percentage of clay is low (1-3 %), d50 values are in 2-12 mm size-fraction, and clasts are mainly subangular. One till sample (material below 64 mm) taken during the field control from the down-ice margin of a triangular landform (Figs 5c and 6A) also indicates low content of clay and silt fraction (3.3 %) and the d50 value is in fine gravel. The tills are generally bouldery and very hard to dig. A special feature of the two test pits in the Kynäsjärvi area is a 10-20 cm thick sand horizon separating two sandy/gravelly till beds (Fig. 12). During the field control an existing 4.5 m deep pit excavated into a bouldery till hummock near a triangular landform within the Harjakangas S site (3) was documented (Fig. 13). In accordance with the Kynäsjärvi sites, the deposits in the Harjakangas S site reveal gravelly and sandy till beds separated by a sand layer. Moreover, four slightly different units of till were identified from the Harjakangas S sediment log as presented in figure 13.

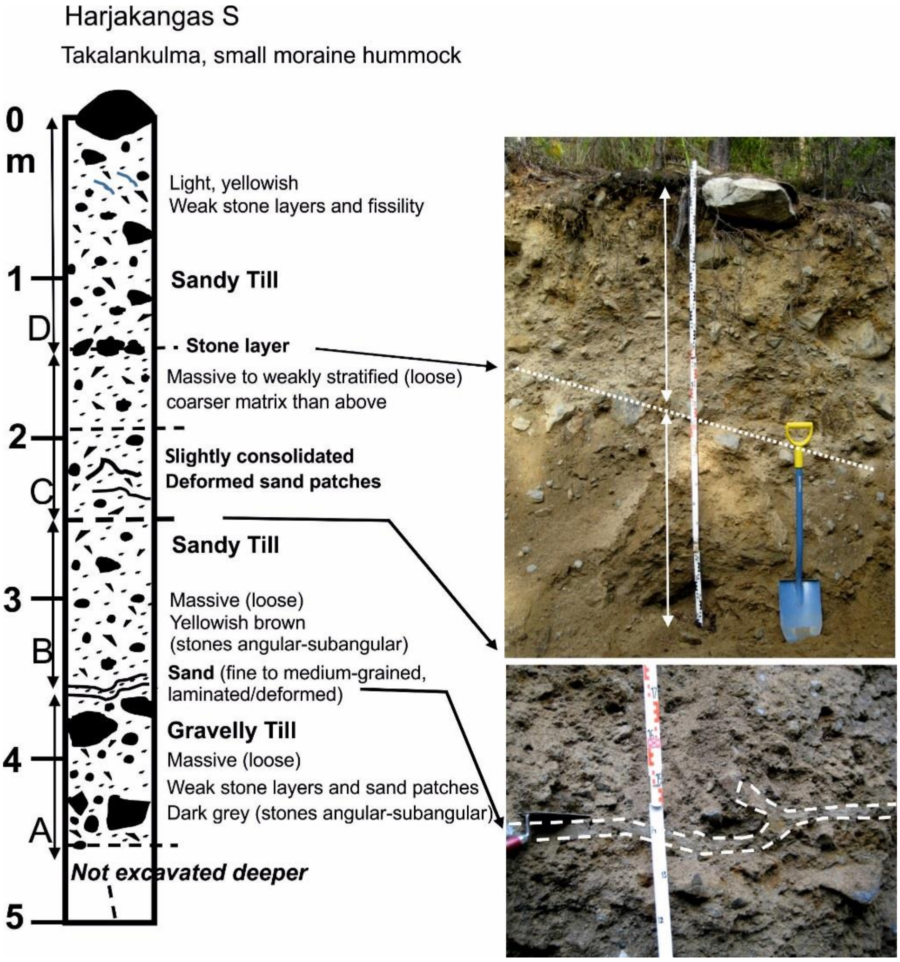

Fig. 13. Sedimentological log from the Harjakangas S site. The site located down-ice from a fan-shaped hollow. Note the intervening sand layer between till beds A and B (lower photo). The upper photo shows the two slightly different till beds (C and D) in upper part of the log. (1,5 column image)

Based on the few roadside excavations, the tills of the Murtoo system are composed of both structureless sandy till and clayey till (Fig. 11). The sandy tills show occasional rafts of clay and clasts surrounded by hardened fine-grained material. However, the internal composition of the low escarpments is not yet adequately documented and more sedimentological research is required to fully understand their origin.

4.4. Distribution of the triangular landforms in SW Finland

4.4.1. The major Satakunta hummocky moraine terrain (HMT)

The Satakunta HMT is located on the eastern side of the Satakunta sandstone depression separated by a 10 km wide basement rock shear zone. The eastern margin of the shear zone and the western margin of the hummocky moraine terrain is delineated by the long NNW-SSE oriented Ahlainen-Forssa esker that continues until the Ss III ice-marginal complex. The Poosjoki-Sääksjärvi route follows the eastern side of the esker. The Satakunta HMT is mostly lacking eskers as indicated by the map of Quaternary deposits. Based on LiDAR data, most landforms within the Satakunta HMT consist of varied ribbed moraines and low relief hummocks. Weakly developed streamlined fields exist only as few scattered patches.

Two long geomorphologically distinguishable routes (Poosjoki-Sääksjärvi and Kynäsjärvi-Jokihaara) associated with well-developed triangular landforms constitute the margins of the hummocky moraine terrain and are subsequently associated with eskers that start from the SE margin of the area (Fig. 2). The overall landform record within the Satakunta HMT might relate to the deposition, deformation and erosion at different stages during the deglaciation. Therefore, more detailed interpretation of the deglacial processes and their chronology cannot be done without detailed geomorphological mapping and sedimentological evidence.

4.4.2. Relationship with major eskers and bedrock fracture valleys

Three long eskers have their origin at the SE end of the Satakunta HMT area which is located about 100 km NW of the Ss III ice-marginal complex (Fig. 1). These eskers are associated with the major geomorphological routes with triangular landforms (sites 8, 9 and 15). Two of the eskers have their origin close to the Lake Sääksjärvi. The appearance of the eskers is related to the start of the major drumlin fields to the SE of the Huittinen-Sastamala area (Fig. 1). Further towards the SE drumlins and tributary eskers become more common. The Kynäsjärvi-Jokihaara route ends in the lake Karhijärvi that forms the onset area for a long tributary Lavia-Nokia esker that follows narrow and deep lake basins feeding the major Pälkäne-Tampere interlobate esker (Fig. 2). Furthermore, this route is associated with the distinct local E-W striations towards the Tampere interlobate system.

The most evident route with triangular landforms is the Ylistenjärvi route (SE of the Satakunta HMT area) ending about 80 km from the Ss III ice-marginal complex (Fig. 2, sites 10-11). The triangular landforms associated with the low escarpments outside the major routes are located at the margins of the major bedrock fracture valleys (sites 16-18, Fig. 2). East of Sastamala (sites 16 and 17), low escarpments show a transition to the onset of the 50-60 km long Ramsöö-Hämeenlinna esker (Fig. 2). This esker delineates the boundary between the eastern margin of the III Salpausselkä flow stage and the ice flow corridor to the SW of the Pälkäne-Tampere interlobate complex.

5. Discussion

5.1. The origin of the triangular landforms

Characteristics of the subglacial distributed drainage are relatively well theorized and modeled in the scientific literature, but representative templates with detailed information on size, geomorphology and sediment characteristics from subglacial paleo-bed records have not emerged (cf. Greenwood et al., 2016). The high-resolution LiDAR DEM data over wide areas of past subglacial beds offers now an unprecedented tool to study the often relatively subtle traces left behind by subglacial water flow as well as deforming till.

The morphological and sedimentological characteristics as well as the distribution of the triangular-shaped till landforms, small till ridges, fan-shaped hollows and channels are interpreted to indicate an origin that involves the creep of saturated deforming till as well as the flow and pressure fluctuations of subglacial meltwater associated with meltwater erosion (Fig. 14). The lack of deposits composed of sorted sediments and rounded clasts is interpreted to show shifting of short-lived meltwater flow with short transport distances in association with contemporaneous creep of saturated till.

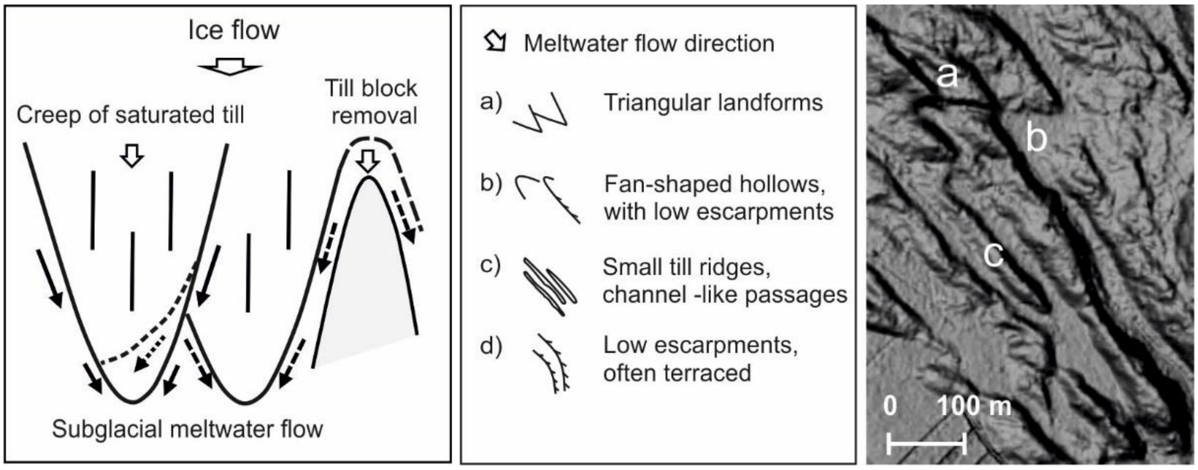

Fig. 14. Left: Schematic drawing of side-lapping triangular landforms. The landforms show erosional slopes by till block removal and meltwater erosion. Subglacial meltwater flow is indicated with arrows, Middle: Characteristic morphological features for recognizing subglacial drainage, Right: These features are often occurring together forming morphologically distinguishable routes. The LiDAR image from the site 5, Joutsijärvi. LiDAR © National Land Survey of Finland. LiDAR processing © Geologian tutkimuskeskus. (2 column image)

We suggest that the regularly fan-shaped hollows and related erosional slopes of the triangular landforms have been initiated by the removal of till blocks and subsequent erosion by subglacial meltwater flow along the down-ice margins (Fig. 14). This could point to the localized refreezing and pressure fluctuations of subglacial water flow. Recently, Seppälä (2016) described triangular patterns related to the fan-like hollows of glacial raft or fan-like edges and steps of plucked hollows in the till bed, which he has interpreted glaciotectonic features. This would imply that the hollows have been produced as rafts associated with the frozen bed conditions. However, the close association with geomorphologically distinquishable routes and the distribution of small channels indicate that the triangular landforms and associated fan-shaped hollows are a part of comprehensive subglacial drainage systems. This is also evidenced by the small and separate Ameenjärvi system close to the start of an esker (Fig. 9).

Importantly, Hooke and Fastook (2007) concluded that the elevated basal temperature gradient occurs within the area of distributed drainage and the restricted esker formation in conduits due to the inhibited melting up into the ice even a few tens of kilometers from the ice margin. This could explain the localized refreezing of till into the overlying ice thus promoting the formation of fan-shaped hollows by the ice flow. Nevertheless, we cannot exclude the possibility that the genesis of the fan-shaped hollows is triggered by the flow of meltwater through the saturated till. The role of refreezing conditions in the development of the triangular landforms and related fan-shaped hollows needs further research.

When the amount of water increased within the routes, the removed till became saturated leading to the creep of till and flow of excess meltwater. The down-ice slopes of triangular landforms are interpreted to show erosion by meltwater flow. The partly fan-shaped hollows (pockets) between the till forms and channels were probably filled with water at this stage (cf. Hooke and Pohjola, 1994). The creep of till is also evidenced by side-lapping triangular forms and different till beds with sand and gravel patches separated by sorted layers. Also varying erosional and depositional patterns imply shifting drainage conditions along the routes.

Short boulder ridges on top of the triangular landforms (Fig. 6 E, F), resembling fluted surfaces to some extent, are interpreted to indicate ice flow. The low channels are interpreted to show the presence of meltwater flow. The high amount of boulders within the drainage routes is probably due to the high transport rates of deforming till associated with meltwater erosion and/or related to subglacial channel armoring that leads to upward meltwater incision into the ice (cf. Lee et al., 2015). However, the more detailed formation process cannot yet be evoked.

There are no existing models for the formation of this kind of large-scale distributed drainage route systems. However, they are interpreted to represent abundant and varying meltwater delivery in association with the creep of saturated deformation till. We tentatively suggest that such landform patterns could be comparable to the linked-water-pocket drainage systems with meltwater pressure fluctuations (cf. Engelhardt and Kamb, 1997; Hooke, 2005), but in much larger scale than presented so far (cf. Hooke, 2005).

In the steady state, the creep of till into a conduit must have been balanced by the erosion of till due to the flow of meltwater (Alley, 1989; Walder and Fowler, 1994; Ng, 2000; Hooke, 2005). The transverse change in the triangular landform morphology over the routes shows that the meltwater discharge and the related erosion was concentrated along the main flow paths generating the most pronounced and sharply delineated triangular landforms. This probably indicates that the smaller scale distributed drainage was collected to these larger scale routes and then finally towards the channelized tunnel flow in the subglacial environment of lower pressure conditions (cf. Hooke, 2005).

The Kynäsjärvi and Harjakangas sandy and gravelly tills with sandy horizons deviate from the material characteristics to the rest of the test pits within the Satakunta HMT area and provide further evidence for the routed subglacial drainage and saturated tills. The intervening sand layers between the different till beds indicate a meltwater flow stage followed by the renewed motion of till (cf. Salomon, 2015). The Kynäsjärvi E site shows less well developed triangular patterns, which may indicate a higher role of meltwater flux on the more rigid bed compared to the areas with thicker deposits of the deforming till. The varying till properties of the smaller Murtoo system with low escarpments suggests that the associated deforming till is sandy, whereas places with subglacial erosion reveal more clayey tills. However, more continuous trenches dug into these landforms are needed to confirm their sedimentological characteristics as well as the mode of the sediment transport and deposition. In addition, the local and restricted erosional role of the shore processes during the glacio-isostatic land uplift must be considered especially for washed slopes and ridges as well as bouldery surfaces.

The low escarpments and drainage patterns with less pronounced triangular landforms probably indicate that meltwater flow and related erosion were associated with the slow movement of deforming till. Small till ridges are interpreted to represent mainly erosional remnants of deforming till along the narrowing drainage route. Similar landform features have been observed in Ostrobothnia close to the Bothnian Sea, where they co-exist with ribbed moraine fields at the shear margins of ice flow corridors and as continuations of the eskers that terminate in hummocky moraine bands (cf. Ahokangas and Mäkinen, 2014). Large part of the material transported by the subglacial meltwater along the described drainage routes was deposited along the major bedrock fracture valleys, eskers and proposed subglacial lakes, whereas more fine-grained materials were transported through the subglacial drainage system into the ice-marginal water bodies forming varved clays.

The spreading of the triangular landforms towards east between sites 2-5 show their linkage to ribbed moraines, but a clear landform continuum cannot be found. It is possible that the meltwater from the routes spread side wards and over a wider area at some point during the deglaciation. Deglacial changes and relationship between triangular landforms and ribbed moraines must be better investigated in other ice lobe areas before embarking further explanations.

The elevated subglacial water pressure in distributed drainage can promote sliding (Gulley et al., 2012) and a high erosion potential of fast flowing ice (Livingstone et al., 2015). It also seems evident that bedrock fracture valleys and probably some of the current lake basins held subglacial water bodies that contributed to fast sliding conditions during the deglaciation. Similarly, the Rutford Ice Stream in Antarctica is likely associated with a patchy mosaic (kilometer-scale) of saturated deforming sediments and ponded water bodies (e.g. King et al., 2004; Smith et al., 2007; Murray et al., 2008). Furthermore, we have preliminary evidence that subglacial lakes existed between the Ss III ice-marginal complex and the distributed drainage routes of the Satakunta HMT (Kajuutti et al., 2016). However, the research into their identification is in its infancy (cf. Greenwood et al., 2016). On the other hand, it is well known that the Antarctic ice sheet contains hundreds of subglacial lakes (Livingstone et al., 2013), therefore it is plausible that the rapidly melting Scandinavian ice sheet would also have been characterized by subglacial lakes and small water bodies. Subglacial lakes in Greenland have been reported by Palmer et al. (2013), Willis et al. (2015), and Howat et al. (2015).

The routed subglacial drainage system evolved during the conditions of rapid deglaciation and melting of the continental ice sheet, thus forming an environment that is not comparable to the modern ice sheet environments. Because the described subglacial distributed drainage routes with large-scale erosional features were providing meltwater for the channelized flow in tunnels with high meltwater volumes, we claim that the subglacial drainage features with triangular landforms must be considered to represent an efficient drainage system for the subglacial meltwater transfer. This would also explain the unresolved problem how tunnels extend themselves headward during the deglaciation (cf. Banerjee and McDonald, 1975; Hooke and Fastook, 2007). There is increasing evidence for efficient drainage in high pressure settings (Fudge et al. 2008), and our observations are supported by Meierbachtol et al. (2013) who “surmise that, toward the ice sheet interior, a network of efficient distributed pathways develops in contrast to large melt channels”. Carter (2008) concluded that a distributed system with discharges of several tens of cubic meters per second should be hundreds of meters wide and tens of centimeters deep. Thus, the dimensions of the triangular landforms and related erosional features proposed in the present study might indicate a discharge of hundreds of cubic meters per second.

5.2. Relationship between triangular landforms and eskers

We contribute to the apparent demand of topologies, drainage processes and geomorphological products of the subglacial drainage (Fig. 14) (cf. Greenwood et al., 2016). Importantly, we describe the transition from broad erosional meltwater systems to single meltwater conduits represented by the esker deposition, which is one of the least solved themes in the current glaciodynamic research (Flowers et al., 2005; Clerc et al., 2012). This problem relates to the operational length of subglacial channels that has remained uncertain. It might be due to the fact that the modern ice sheets are inappropriate analogues, because their hydrological conditions are different from those during the rapid deglaciation of mid-latitude ice sheets (cf. Greenwood et al., 2016). However, recent research comparing esker paths and numerically modelled subglacial drainage routes suggests that eskers form within <10 km distance from the ice margin (cf. Livingstone et al., 2015). The downstream transition from the routes with triangular-shaped landforms into eskers demonstrates a switch from the sediment erosion to deposition (cf. Livingstone et al., 2016).

The Satakunta hummocky moraine terrain was likely nearing stagnant conditions during the deglaciation after the last flow stage related to the formation of the Ss III ice-marginal complex. This is evidenced by the lack of eskers and related glaciofluvial landforms, the preservation of subglacial drainage features and the lack of drumlin fields in this area. The triangular landforms closest to the Ss III are located at about 45-60 km distance in association with the upstream area of the Urjala-Akaa subglacial lake. This distance coincides with the end of several distinctive and continuous eskers starting from the Salpausselkä complex. Similar distance applies for the transition from the routes with triangular landforms to the Lavia-Nokia esker, and for the fracture valley systems west of the Pälkäne-Tampere interlobate esker. In order to explain the high volumes of meltwater in subglacial drainage system over 50 km from the grounding line, the substantial melting of the proposed stagnating ice within the Baltic Sea ice lobe margin must be considered (cf. Carlson et al., 2009).

The last ice-marginal position during the deglaciation reflected by the esker patterns and ice-marginal till ridges occurs along the Urjala-Loimaa line. The area behind this position shows the termination of two eskers at the distance of 50-60 km in association with the change to the triangular landform patterns within the Satakunta HMT. The only esker that continues further NW over longer distances is the non-dendritic Ahlainen-Forssa esker that forms the western boundary of the Satakunta HMT along the NW-SE bedrock shear zone. The western arc of the CFIMF forms the NE margin of the Baltic Sea ice lobe. The sedimentology of the Somero-Pori interlobate esker bordering the study area towards the west along the Satakunta NW-SE sandstone contact suggests time-transgressive deposition with high seasonal variation (Mäkinen, 2003b) that is probably connected to the supraglacial meltwater input.

Based on the above-mentioned evidence, we suggest that the distance of the conduit dominated drainage in transition to the distributed drainage with a deforming bed was about 50-60 km from the margin, but that the final sedimentation in the tunnels took place closer. This distance with the low-pressure conditions and channelized drainage is supported by the observations from the modern ice sheets (Bartholomew et al., 2011a,b; Chandler et al., 2013; Schroeder et al., 2013) and numerical modelling results (Meierbachtol et al., 2013; Dow et al., 2014). Furthermore, Greenwood et al. (2016) conclude that the weight of evidence supports a spatial extent of a dendritic channelized topology (cf. Röthlisberger, 1972) limited to about 50 km. However, they also speculate that in some conditions it may be possible for the conduits to extend over longer distances under high pressure and likely appear as a non-dendritic system. The scarcity of the drainage systems with triangular landforms within the fast flow of ice streams is likely explained by their poor preservation potential.

6. Conclusions

Our hypothesis is that the subglacial drainage routes with triangular landforms described herein form a transitory drainage between channelized (eskers) and more widely spread small-scale distributed drainage systems. They represent efficient subglacial meltwater drainage under high pressure conditions partially associated with the till block removal and the creep of the deforming till. In such case, our findings enhance the understanding of deglacial dynamics and the streaming ice flow within the Scandinavian Ice Sheet.

We describe previously poorly identified landforms and landform associations that help to facilitate the interpretation of the paleo-record of deforming beds with the distributed drainage on past subglacial beds. The role of subglacial meltwater activity had a more prominent effect on the formation of subglacial landforms and the related behavior of the ice flow than was previously understood. However, the preservation potential of the triangular landforms within the fast flow of the ice streams is likely low. We strongly agree with Greenwood et al. (2016), who stated that the ice sheet hydrology is a poorly incorporated component of the palaeo-glaciological models, which thus should be carefully re-evaluated. We provide an important contribution towards a more realistic representation of the hydrological drainage systems within the ice sheets. Furthermore, it could be used when simulating the likely responses of the ice sheets to the increased meltwater production.

Importantly, current results also suggest that a marked increase in the subglacial meltwater volume and the related change in deforming bed conditions due to the warming climate within the Greenland ice sheet could lead to the ice sheet instability with serious consequences for the present ocean currents, the global climate system and the sea level change. It is generally accepted that the past mid-latitude ice sheets were characterized by a strong supraglacial meltwater production that must find its way to the subglacial environment at some distance from the grounding line. As stated by Greenwood et al. (2016), we should better understand "the dynamic responses of ice flow to hydrological processes, and to better predict likely responses of ice sheets and ice sheet sectors to increased surface melting under atmospheric warming scenarios".

Acknowledgements

We wish to thank Dr. Niko Putkinen for the support and discussions related to the collaboration on glacial dynamics of Finland between the University of Turku and the Geological Survey of Finland. We are grateful to Sarah Greenwood and one anonymous reviewer for their constructive and critical comments and improvement of the manuscript.

This research did not receive any specific grant from funding agencies in the public, commercial, or not-for-profit sectors.

References

Ahokangas, E., Mäkinen, J. 2014. Sedimentology of an ice margin esker with implications for the deglacial dynamics of the Finnish Lake District lobe trunk. Boreas 43, 90–116.

Alley, R.B. 1989. Water pressure coupling of sliding and bed deformation. I. Water System. J. Glaciol. 35, 108–118.

Ashmore, D.W., Bingham, R.G. 2014. Antarctic subglacial hydrology: an overview of current knowledge and forthcoming scientific challenges. Antarctic Science 26, 758–773.

Banerjee, I., McDonald, B.C. 1975. Nature of esker sedimentation, In: Jopling, A.V., McDonald, B.C., (eds.), Glaciofluvial and glaciolacustrine sedimentation. Society of Economic Paleontologists and Mineralogists, Special Publication 23, Tulsa, Oklahoma, U.S.A., 132-154.

Bartholomew, I., P. Nienow, A. Sole, D. Mair, T. Cowton, and M. King 2011a. Seasonal variation in Greenland Ice Sheet motion: Inland extent and behaviour at higher elevations, Earth Planet. Sci. Lett., 307, 271–278.

Bartholomew, I., P. Nienow, A. Sole, D. Mair, T. Cowton, S. Palmer, and J. Wadham 2011b. Supraglacial forcing of subglacial drainage in the ablation zone of the Greenland ice sheet, Geophys. Res. Lett. 38, L08502.

Beem, L.C., Jezek, K.C., Van Der Veen, C.J. 2010. Basal melt rates beneath Whillans Ice Stream, West Antarctica. J. Glaciol. 56, 647–654.

Boulton, G.S., Dongelmans, P., Punkari, M., Broadgate, M., 2001. Palaeoglaciology of an ice sheet through a glacial cycle: the European ice sheet through the Weichselian. Quat. Sci. Rev. 20, 591–625.

Boulton, G.S., Hagdorn, M., Malliot, P.B., Zatsepin, S., 2009. Drainage beneath ice sheets: groundwater–channel coupling, and the origin of esker systems from former ice sheets. Quat. Sci. Rev. 28, 621–638.

Carlson A.E., Anslow F.S., Obbink E.A., LeGrande A.N., Ullman D.J., Licciardi J.M., 2009. Surface-melt driven Laurentide Ice Sheet retreat during the early Holocene: Geophys. Res. Lett. 36, L24502.

Carter, S.P., 2008. Evolving Subglacial Water Systems in East Antarctica from Airborne Radar Sounding. Dissertation. The University of Texas at Austin. 241 pp.

Chandler, D.M., Wadham, J.L., Lis, G.P., Cowton, T., Sole, A., Bartholomew, I., Telling, J., Nienow, P., Bagshaw, E.P., Mair, D., Vinen, S., Hubbard, A., 2013. Evolution of the subglacial drainage system beneath the Greenland Ice Sheet revealed by tracers. Nat. Geosci. 6, 195–198.

Clark, P.U., Walder, J.S. 1994. Subglacial drainage, eskers, and deforming beds beneath the Laurentide and Eurasian ice sheets. Geol. Soc. Am. Bull. 106, 304–314.

Clerc, S., Buoncristiani, J.-F., Guiraud, M., Desaubliaux, G., Portier, E. 2012. Depositional model in subglacial cavities, Killiney Bay, Ireland. Interactions between sedimentation, deformation and glacial dynamics. Quat. Sci. Rev. 33, 142–164.

Cowton, T., Nienow, P., Sole, A., Barthoholomev, I., Mair, D. 2016. Variability in ice motion at a land-terminating Greenlandic outlet glacier: the role of channelized and distributed drainage systems. J. Glaciol. 62, 451-466.

Dow, C.F., Kulessa, B., Rutt, I.C., Doyle, S.H., Hubbard, A. 2014. Upper bounds on subglacial channel development for interior regions of the Greenland ice sheet. J. Glaciol. 60, 1044–1052.

Engelhardt, H., Kamb, B., 1997. Basal hydraulic system of aWest Antarctic ice stream: constraints from borehole observations. J. Glaciol. 43, 207–230.

Evans, D.J.A., Phillips E.R., Hiemstra, J.F., Auton, C.A. 2006. Subglacial till: Formation, sedimentary characteristics and classification. Earth-Sci. Rev. 78, 115–176.

Flowers, G.E., Björnsson, H., Pálsson, F., 2003. New insights into the subglacial and periglacial hydrology of Vatnajökull, Iceland, from a distributed physical model. J. Glaciol. 49, 257–270.

Flowers, G.E., Björnsson, H., Pálsson, F., Clarke, G.K.C. 2004. A coupled sheet-conduit model of jökulhlaup propagation. Geophys. Res. Lett. 31.

Flowers, G.E., Marshall, S.J., Björnsson, H., Clarke, G.K.C. 2005. Sensitivity of Vatnajökull ice cap hydrology and dynamics to climate warming over the next two centuries. J. Geophys. Res. 110.

Fudge, T., Humphrey, N., Harper, J., and Pfeffer, W., 2008. Diurnal fluctuations in borehole water levels: configuration of the drainage system beneath Bench Glacier, Alaska, USA. J. Glaciol., 54, 297–306.

Geological Survey of Finland, 2016. Map of Superficial deposits in Finland 1:1 000 000. Geologian tutkimuskeskus (GTK) 2016.

Greenwood, S.L., Clason, C. C., Helanow, C.,Margold, M. 2016a. Theoretical, contemporary observational and palaeo-perspectives on ice sheet hydrology: Processes and products. Earth Sci. Rev. 155, 1–27.

Gulley, J.D., Grabiec, M., Martin, J.B., Jania, J., Catania, G., Glowacki, P., 2012. The effect of discrete recharge by moulins and heterogeneity in flow-path efficiency at glacier beds on subglacial hydrology. J. Glaciol. 58, 926–940.

Hewitt, I.J. 2011. Modelling distributed and channelized subglacial drainage: the spacing of channels. J. Glaciol. 57, 302–314.

Hooke, R. LeB, Pohjola, V. A. 1994. Hydrology of a segment of a glacier situated in an overdeepening, Storglaciaren, Sweden. J. Glaciol. 40, 140–148.

Hooke, R. LeB 2005. *Principles of Glacier Mechanics*. 429 pp. Cambridge University Press, Cambridge.

Hooke, R. LeB, Fastook, J. 2007. Thermal conditions at the bed of the Laurentide ice sheet in Maine during deglaciation: implications for esker formation. J. Glaciol. 53, 646–658.

Howat, I. M., Porter, C., Noh, M.J., Smith, B.E., Jeong, S. 2015. Brief Communication: Sudden drainage of a subglacial lake beneath the Greenland Ice Sheet. Cryosphere 9, 103–108.

Hughes, A.L.C., Gyllencreutz, R., Lohne, Ø.S., Mangerud, J., Svendsen, J.I., 2016. The last Eurasian ice sheets – a chronological database and time-slice reconstruction, DATED-1. Boreas 4, 1–45.

Humphrey, N.F., 1987. Coupling between water pressure and basal sliding in a linked-cavity hydraulic system. The Physical Basis of Ice Sheet Modelling (Proceedings of the Vancouver Symposium, August 1987). IAHS Publ. no. 170.

Jenness, J., 2013: *DEM surface tools. Jenness enterprises*. Available at: http://www.jennessent.com/arcgis/surface_area.htm

Johnson, M.D., Fredin, O., Ojala, A.E.K., Peterson, G. 2015. Unraveling Scandinavian geomorphology: the LiDAR revolution, GFF 137, 245–251.

Kangas, K. 2003. Elämisen ehtoja Kankaanpään Karvianjokilaaksossa. Kulttuurituotannon ja maisemantutkimuksen laitos, Turun yliopisto. University of Turku, 13.5.2003.

Kajuutti, K., Mäkinen, J., Palmu, J.-P. 2016. LiDAR-based interpretation of deglacial dynamics in SW Finland, In: Staubolis, S., Karvonen, T., Kujanpää, A. 2016. Abstracts of The 32 nd Nordic Geological Winter Meeting 13th-15th January 2016, Helsinki, Finland. Bull. Geol. Soc. Finl. 314.

King, E.C., Woodward, J.M., Smith, A.M. 2004. Seismic evidence for a water-filled canal in deforming till beneath Rutford Ice Stream, West Antarctica. Geophys. Res. Lett. 31, L20401.

Kujansuu, R., Niemelä, R., (Eds.) 1984. Quaternary deposits of Finland I: 1 000 000. Geological Survey of Finland, Espoo.

Lee, J.R., Wakefield, O.J.W., Phillips, E., Hughes, L. 2015. Sedimentary and structural evolution of a relict subglacial to subaerial drainage system and its hydrogeological implications: an example from Anglesey, north Wales, UK. Quat. Sci. Rev. 109, 88–110.

Lehtinen, M., Nurmi, P., Rämö, T., (Eds.) 2005. Precambrian geology of Finland: key to the evolution of the Fennoscandian Shield. Developments in Precambrian geology 14, Elsevier, Amsterdam, 736 pp.

Livingstone, S.J., Clark, C.D., Woodward, J., Kingslake, J. 2013. Potential subglacial lake locations and meltwater drainage pathways beneath the Antarctic and Greenland ice sheets. Cryosphere 7, 1721–1740.

Livingstone, S.J., Storrar, R.D., Hillier, J.K., Stokes, C.R., Clark, C.D., Tarasov, L. 2015. An ice-sheet scale comparison of eskers with modelled subglacial drainage routes. Geomorphology 246, 104–112.

Livingstone, S.J., Utting, D.J., Ruffell, A., Clark, C.D., Pawley, S., Atkinson, N., Fowler, A.C. 2016. Discovery of relict subglacial lakes and their geometry and mechanism of drainage. Nature Commun. 7:11767.

Lunkka, J.P., Johansson, P., Saarnisto, M., Sallasmaa, O., 2004. Glaciation of Finland, In: Ehlers, J., Gibbard, P.L., (eds.), Quaternary glaciations – Extent and chronology. Elsevier, Amsterdam, 93–100.

Meierbachtol, T., J. Harper, and N. Humphrey 2013. Basal drainage system response to increasing surface melt on the Greenland ice sheet. Science, 341, 777–779.

Murray, T., Corr, H., Forieri, A., Smith, A.M., 2008. Contrasts in hydrology between regions of basal deformation and sliding beneath rutford Ice stream, West Antarctica, mapped using radar and seismic data. Geophys. Res. Lett. 35, L12504.

Mäkinen, J. 2003a. Development of depositional environments within the interlobate Säkylänharju-Virttaankangas glaciofluvial complex in SW Finland. Ann. Acad. Sci. Fenn. Geol.-Geogr. 165. 65 pp.

Mäkinen, J. 2003b. Time-transgressive deposits of repeated depositional sequences within interlobate glaciofluvial (esker) sediments in Köyliö, SW Finland. Sedimentology 50, 327–360.

Ng, F.S.L., 2000. Canals under sediment-based ice sheets. Ann. Glaciol. 30, 146–152.

Ojala, A.E.K., Palmu, J.-P, Åberg, A., Åberg, S., Virkki, H., 2013. Development of an ancient shoreline database to reconstruct the Litorina Sea maximum extension and the highest shoreline of the Baltic Sea basin in Finland. Bull. Geol. Soc. Finl. 85, 127–144.

Ojala, A.E.K., 2016. Appearance of De Geer moraines in southern and western Finland – implications for reconstructing glacier retreat dynamics. Geomorphology 255, 16–25.

Palmer, S.J., Dowdeswell, J.A., Christoffersen, P., Young, D. A., Blankenship, D.D., Greenbaum, J.S., Benham, T., Bamber, J., Siegert, M.J. 2013. Greenland subglacial lakes detected by radar. Geophys. Res. Lett. 40, 6154–6159.

Phillips, E., Lee, J.L. 2013. Development of a subglacial drainage system and its effect on glacitectonism within the polydeformed Middle Pleistocene (Anglian) glacigenic sequence of north Norfolk, Eastern England. Proc. Geol. Assoc. 124, 855–875.

Röthlisberger, H. 1972. Water pressure in intra- and subglacial channels. J. Glaciol. 11:62, 177–203.

Saarnisto, M., Lunkka, J.P., 2004. Climate variability during the last interglacial-glacial cycle in NW Eurasia, In: Battarbee, R.W., Gasse, F., Stickley, C.E., (eds.), Past climate variability through Europe and Africa. Developments in Paleoenvironmental Research 6, Springer, Dordrecht, 443–464.

Salamon, T. 2015. Subglacial conditions and Scandinavian Ice Sheet dynamics at the coarse-grained substratum of the fore-mountain area of southern Poland. Quat. Sci. Rev. 151, 72–87.

Salonen, V.-P., 1986. Glacial transport distance distributions of surface boulders in Finland. Bull. Geol. Surv. Finl. 338, 57 pp.

Sauramo, M. 1923. Studies on the Quaternary varve sediments in southern Finland. Bull. Comm.Géol. Finl. 60.

Shreve, R.L. 1985. Esker characteristics in terms of glacier physics, Katahdin esker system, Maine. Geol. Soc. Am. Bull. 96, 639–646.

Seppälä M.V.J. (2016). Lidar-Based Detection and Interpretation of Glaciotectonic Features of the Morainic Topography of Finl. J. Geol. Res. 2016, 11 p.

Schroeder, D.M., Blankenship, D.D., Young, D.A. 2013. Evidence for a water system transition beneath Thwaites Glacier, West Antarctica. Proc. Natl. Acad. Sci. U. S. A. 110, 12225–12228.

Smith, A. M., Murray, T., Nicholls, K. W., Makinson, K., Aoalgeirsdottir, G., Behar, A. E., and Vaughan, D. G., 2007. Rapid erosion, drumlin formation, and changing hydrology beneath an Antarctic ice stream, Geology 35, 127–130.

Stroeven, A.P., Hättestrand, C., Kleman, J., Heyman, J., Fabel, D., Fredin, O., Goodfellow, B.W., Harbor, J.M., Jansen, J.D., Olsen, L., Caffee, M.W., Fink, D., Lundqvist, J., Rosqvist, G.C., Strömberg, B., Jansson, K.N., 2016. Deglaciation of Fennoscandia. Quat. Sci. Rev. 147, 91–121.

Svendsen, J.I., Alexanderson, H., Astakhov, V.I., Demidov, I., Dowdeswell, J.A., Funder, S., Gataullin, V., Henriksen, M., Hjort, C., Houmark-Nielsen, M., Hubberten, H.W., Ingólfsson, Ó., Jakobsson, M., Kjær, K.H., Larsen, E., Lokrantz, H., Lunkka, J.P., Lyså, A., Mangerud, M., Matiouchkov, A., Murray, A., Möller, P., Niessen, F., Nikolskaya, O., Polyak, L., Saarnisto, M., Siegert, C., Siegert, M.J., Spielhagen, R., Stein, R., 2004. Late Quaternary ice sheet history of northern Eurasia. Quat. Sci. Rev. 23, 1229–1271.

Walder, J.S., Fowler, A. 1994. Channelized subglacial drainage over a deformable bed. J. Glaciol. 40, 3–15.

Willis, M.J., Herried, B.G., Bevis, M.G. & Bell, R.E. 2015. Recharge of a subglacial lake by surface meltwater in northeast Greenland. Nature 518, 223–227.